Ultramicroscopy 182 (2017) 169–178

Contents lists available at ScienceDirect

Ultramicroscopy

journal homepage: www.elsevier.com/locate/ultramic

Measuring nanometre-scale electric fields in scanning transmission electron microscopy using segmented detectors

H.G. Brown[a], N. Shibata[b], H. Sasaki[c], T.C. Petersen[a], D.M. Paganin[a], M.J. Morgan[a], S.D. Findlay[a,*]

[a] *School of Physics and Astronomy, Monash University, Victoria 3800, Australia*
[b] *Institute of Engineering Innovation, School of Engineering, University of Tokyo, Tokyo 113-8656, Japan*
[c] *Yokohama R&D Lab, Furukawa Electric Ltd., Yokohama 220-0073, Japan*

ARTICLE INFO

Article history:
Received 6 April 2017
Revised 28 June 2017
Accepted 2 July 2017
Available online 3 July 2017

Keywords:
Scanning transmission electron microscopy (STEM)
Differential phase contrast (DPC) imaging
p-n junctions
Electric fields

ABSTRACT

Electric field mapping using segmented detectors in the scanning transmission electron microscope has recently been achieved at the nanometre scale. However, converting these results to quantitative field measurements involves assumptions whose validity is unclear for thick specimens. We consider three approaches to quantitative reconstruction of the projected electric potential using segmented detectors: a segmented detector approximation to differential phase contrast and two variants on ptychographical reconstruction. Limitations to these approaches are also studied, particularly errors arising from detector segment size, inelastic scattering, and non-periodic boundary conditions. A simple calibration experiment is described which corrects the differential phase contrast reconstruction to give reliable quantitative results despite the finite detector segment size and the effects of plasmon scattering in thick specimens. A plasmon scattering correction to the segmented detector ptychography approaches is also given. Avoiding the imposition of periodic boundary conditions on the reconstructed projected electric potential leads to more realistic reconstructions.

1. Introduction

The development of modern materials and devices requires precise control over the electric and magnetic characteristics of these materials and an understanding of how these properties correlate with structural features of the material. Electron microscopy is well suited to characterising these materials. Precise quantification of specimen electric fields has been demonstrated in electron holography [1,2]. However, it would be advantageous if such electric field quantification could also be performed in scanning transmission electron microscopy (STEM), as this would permit simultaneous acquisition of complementary STEM modes for imaging, such as high-angle annular dark-field, and spectroscopic techniques for elemental mapping, such as energy dispersive X-ray analysis.

Differential phase contrast (DPC) STEM has been demonstrated for studies probing magnetic fields at micrometre and nanometre resolutions [3–8], and electric fields at both nanometre [9–12] and atomic [13–15] resolutions. Conceptually, the field within the specimen deflects the trajectory of the electron probe, resulting in a shift of the bright field disk across the diffraction plane. DPC STEM and associated methods seek to use this deflection information to map out the variation of electromagnetic field strength within the sample. This can be done most effectively if the full scattering distribution is available, and the new generation of fast pixel detectors [16–18] provides a means for acquiring the full scattering distribution at each position in a STEM scan raster. However, DPC STEM has to date mostly been undertaken using segmented detectors, which offer sensitivity to beam deflection through the increase in signal in some segments and the decrease in others. This more established technology allows much faster scan speeds and live imaging [11,19], meaning it is still the most practical method for industrial application. However, because segmented detectors only give a coarse sampling of the scattering distribution, more care is required for quantitative analysis. This paper explores several issues that relate to achieving quantitative measurement of nanoscale-electric fields in STEM using segmented detectors.

As our case study, we use DPC STEM data for the GaAs *p-n* junction presented in Ref. [11]. This specimen was 290 nm thick with a symmetrical *p-n* junction between $10^{19}\,\mathrm{cm}^{-3}$ *p*-doped (Zn) and $10^{19}\,\mathrm{cm}^{-3}$ *n*-doped (Si) GaAs. Fig. 1(a) shows unprocessed segmented detector STEM images of this *p-n* junction acquired with a 16 segment JEOL detector [19]. The camera length was chosen

---

* Corresponding author.
E-mail address: scott.findlay@monash.edu (S.D. Findlay).

http://dx.doi.org/10.1016/j.ultramic.2017.07.002
0304-3991/

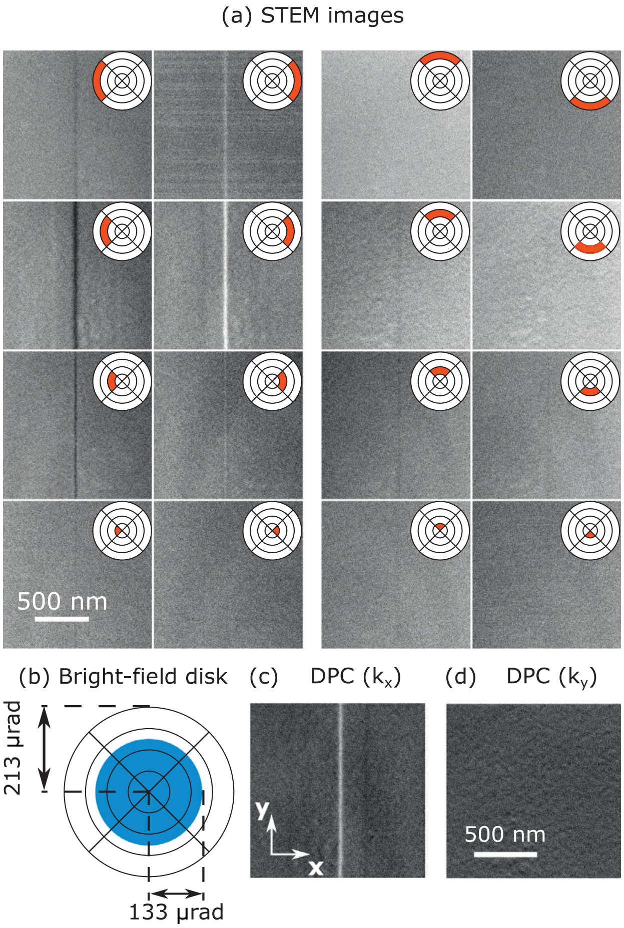

Fig. 1. (a) Unprocessed segmented detector images of a *p*-*n* junction using an accelerating voltage of 200 kV and a 133 μrad probe-forming aperture. The camera length was chosen such that the bright-field disk, represented by a blue circle in (b), sits mid-way through the third ring on the segmented detector. The resultant DPC (i.e. estimated centre of mass) images are shown in (c) and (d). (For interpretation of the references to colour in this figure legend, the reader is referred to the web version of this article.)

such that the bright field disk was situated mid-way through the third annular ring of the segmented detector, as shown schematically in Fig. 1(b). Image contrast at the *p*-*n* junction is clearly visible in the STEM images from the detector segments in the horizontal direction, consistent with the expected increase or decrease in electrons incident upon those segments due to the deflection (towards the right in the figure) of the bright field disk caused by the junction electric field. Faint contrast is also visible for the detector segments in the vertical direction, due to a combination of “absorption contrast” (intensity scattering outside the bright-field disk; hence consistently dark contrast for detectors within the bright field disk), detector inhomogeneity, and residual defocus contrast. Shibata et al. [11] used a model-based analysis to quantify the thickness-integrated electric field strength along the beam direction, which was possible because of the simple geometry of the *p*-*n* junction. However, general reconstruction of field distributions of unknown structure and symmetry requires more direct reconstruction methods. This paper compares three reconstruction approaches, exploring consequences of thick specimens and limitations of implicit assumptions in reconstruction algorithms using a Fourier basis.

The paper is organised as follows. In Section 2 we investigate three methods of reconstructing the *p*-*n* junction projected electric potential and electric field distributions without recourse to a model-based approach: DPC via the first moment or “centre of mass” approach of Waddell and Chapman [20] and Müller et al. [21] as approximated by the segmented detector, and two segmented detector ptychography (SDP) approaches, one due to Brown et al. [22] and the other to Landauer et al. [23]. These methods make potentially limiting assumptions: approximating the centre of mass using segmented detectors in DPC and the weak object approximation in SDP. This means that discrepancies in the quantitative reconstruction of the projected electric field are found when compared with the earlier model-based analysis. In Section 3 we show that by extending the DPC approach using an experimental calibration of the centre of mass response of the detector system we are able to quantitatively retrieve the *p*-*n* junction projected electric field within error bars. We further demonstrate that plasmon scattering contributes appreciably to the required calibration correction, and in Section 4 we show how some of the SDP methods can be modified to account for plasmon scattering. In Section 5 we show how to overcome the distortion that enforcing periodic boundary conditions introduces to the reconstructed potential away from the junction.

2. Reconstruction of the electric field and potential

We will compare three different approaches for reconstructing the projected electrostatic potential of the *p*-*n* junction using the experimental data in Fig. 1. One approach can be used to calculate the electric field information directly, but the other two are phase-retrieval-type approaches, geared towards calculating the projected electrostatic potential, from which the projected electric field can then be determined. The starting point for all three methods is the phase object approximation:

$$\psi_{\text{exit}}(\mathbf{r}, \mathbf{R}) = T(\mathbf{r})\psi_{\text{illum}}(\mathbf{r} - \mathbf{R}), \tag{1}$$

in which ψ_{illum} and ψ_{exit} are wave functions of the incident illumination and the exit surface wave, respectively, with $\mathbf{r}$ denoting the two-dimensional (2D) coordinate in the plane of the sample and $\mathbf{R}$ denoting the probe position in that plane. Neglecting inelastic scattering, the specimen transmission function $T(\mathbf{r})$ is given in terms of the projected electrostatic potential $\overline{V}(\mathbf{r})$ of the system as

$$T(\mathbf{r}) = \exp[i\phi(\mathbf{r})] = \exp\left[\frac{i\pi te\overline{V}(\mathbf{r})}{hv}\right], \tag{2}$$

where t denotes the sample thickness, e is the magnitude of the electron charge, h is Planck’s constant, and v is the relativistically-corrected electron velocity. For atomic resolution imaging with electrons, the phase object approximation is known to break down for specimens that are only a few nanometres thick [21,24], so its application to a 290 nm thick GaAs semiconductor requires justification. Dynamical diffraction in this sample is considerable – almost 98% of the incident electron density has been scattered outside the bright field disk. However, through our choice of camera length, we need only consider the validity of Eq. (1) for the action of the field on that portion of the electron density remaining in and around the bright field region. Gibson [25] suggests that the phase object approximation is reasonable if the criterion $\lambda t k_{\max}^2 \leq 1/4$ is met, in which λ denotes the relativistically-corrected electron wavelength and $k_{\max}$ is the maximum considered magnitude of the 2D diffraction coordinate $\mathbf{k}$ (conjugate to $\mathbf{r}$). This is equivalent to the specimen being thinner than the probe depth of field.[1] For the experiment in Fig. 1, $\lambda = 2.51 \times 10^{-3}$ nm and we conservatively take $k_{\max} = 8.49 \times 10^{-2}\ \text{nm}^{-1}$, which corresponds to a scattering angle of 213 μrad – the extent of our detector system in the

---

[1] It is shown in Ref. [26] that the full-width at half-maximum (FWHM) value for the probe depth of field is given by $\Delta z_{\text{FWHM}} = 1.772/\lambda k_{\max}^2$.